DOI: 10.61782/fa.2025.0689

PREDICTING THE ACOUSTIC RESPONSE OF A RESONANT CAVITY COUPLED TO SONIC BLACK HOLES BY MEANS OF PATCH TRANSFER FUNCTIONS

Pedro Cerântola[1,2*] **Laurent Maxit**[2] **Oriol Guasch**[1] **Jie Deng**[1,3]

[1] Human-Environment Research (HER) group, Department of Engineering, La Salle, Universitat Ramon Llull, C/ Quatre Camins 30, Barcelona, 08022, Catalonia, Spain
[2] Laboratoire Vibrations Acoustique (LVA), INSA Lyon, 25 bis Av. Jean Capelle O, Villeurbanne cedex, 69621, France
[3] Chongqing Industry Polytechnic College, Chongqing, 401120, China

ABSTRACT

Reducing broadband noise in enclosed spaces, such as rooms or the cabins of cars and airplanes, is a challenge for acoustic comfort. In recent years, sonic black holes (SBHs) have been investigated to achieve anechoic terminations in ducts, but their potential for room acoustics remains unexplored. A conventional SBH consists of a wave-guide with concentric inner rings of decreasing radius separated by cavities that are partially filled with absorbing material. This arrangement slows down and traps incident sound waves dissipating their energy, which results in very little reflection beyond the cut-on frequency of the SBH. In this work we study the acoustics of a resonant cavity with an array of SBHs coupled to one of its walls. The patch transfer function (PTF) method is applied to couple the cavity and the set of SBHs. For the former, an analytical modal model is used, while the response of the SBHs is characterized by means of the finite element method (FEM). This substructuring approach provides a low-cost numerical method to investigate how SBH design parameters influence the acoustic response of the cavity.

***Corresponding author**: *pedro.cerantola@salle.url.edu.*

Keywords: *sonic black hole, substructuring method, patch transfer function method, room acoustics, coupled system.*

1. INTRODUCTION

In connection with the need to develop engineering solutions to control vibrations and noise, research in acoustic black holes (ABHs) has been increasing in recent years. In theory, these devices are capable of slowing down impinging elastic waves to a singularity point where the propagation and the reflection become impossible, delivering perfect energy focusing [1]. Two main classes of ABHs are investigated: the vibrational black holes (VBHs), which absorb mechanical vibrations [2, 3], and the sonic black holes (SBHs), that are intended to dissipate sound waves and which were first proposed in [4]. While VBHs consist of thin beams and plates with decreasing thickness profile indentations that can capture and dissipate bending waves, their acoustic counterpart, the SBHs, achieve the black hole effect by means of a waveguide whose inner radius decreases according to a power law profile and whose wall admittance has a specific spatial variation [5]. If a perfectly continuous SBH with a null final radius was possible, perfect absorption could be attained [4, 5].

The most common realization of an SBH is made of a homogeneous wave-guide equipped with various concentric rings of decreasing inner radii that follow the power profile and are separated by cavities. Manufacturing constraints such as the end truncation, number and dimensions of rings and cavities and damping mechanisms will limit the performance of the SBH (see e.g., [6–8]). To date, most works have been devoted to better characterize the SBH as a single system by using different numerical approaches [7, 9, 10] and to enhance its performance at low frequencies using microperforated panels for the cavities [11, 12] or periodic SBHs [13, 14]. Efforts have been also made to optimize the SBH design [15, 16] for a better performance, to find alternative approaches based on metafluid analogies [17, 18] and slow-down lattice absorbers [19], or to design SBH inspired mufflers [20].

However, none of the above works have considered coupling a set of SBHs to a cavity, which could be important for many industrial applications. That is the goal of this paper. Given that aiming at a full finite element method (FEM) simulation of the problem would be computationally very costly, it is herein proposed to resort to a substructuring technique. In this context, the so-called patch transfer function (PTF) is used, which has proven to be very effective in characterizing vibroacoustic systems [21–23]. This method offers a viable option to couple linear subsystems through transfer functions evaluated over patch surfaces at a very low computational cost. We will use the PTF to assess the acoustics of a homogeneous cavity when we couple a set of SBHs to it. The cavity and SBHs will be characterized separately and coupled using continuity conditions in the framework of the PTF [21]. The coupled model will be validated against a full FEM simulation of the complete model.

The main technical aspects of the modelling strategy of the proposed approach are presented in Section 2. The validation of the method is provided in Section 3. Conclusions and future research lines are drawn in Section 4.

2. PTF MODELLING PROCEDURE

2.1 PTF approach to describe the coupling between the cavity and the SBHs

As shown in Fig. 1, let us consider a rectangular cavity with dimensions $L_x \times L_y \times L_z$ coupled to N identical SBHs on face $y = 0$. For simplicity, it is assumed that there is no direct interaction between the SBHs. A monopole source is located inside the cavity at point S of coordinates (x_S, y_S, z_S). Our goal is to predict the mean quadratic pressure inside the cavity taking into account the effect of the SBHs. To this end, we use the PTF substructuring approach to partition the problem into two subsystems. The cavity constitutes one single subsystem whereas the N SBHs constitute the other one. There are N coupling surfaces between the cavity and the SBHs which compose the so-called "patches" in the PTF method (see Fig. 2). The following two conditions must be satisfied:

- the patches must be smaller than than half the acoustic wavelength to respect the PTF criterion, i.e., the frequencies of interest must be lower than a critical frequency corresponding to an acoustic wavelength equal to twice the size of the patch;
- the area of the patches must correspond to that of the opening of the SBHs, but their shapes do not need to be the same. For instance, the opening of the SBH may be in the form of a disk while the patch of the cavity in front of it may be square for convenience. It was shown in the past that this approximation is valid if the previous condition is respected.

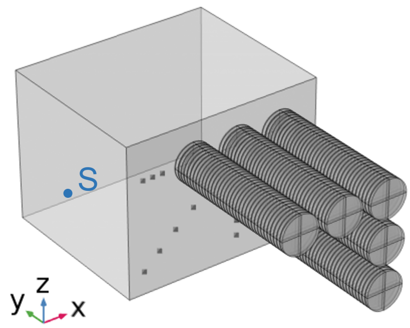

Figure 1. General case of a cavity coupled to N SBHs.

For acoustic domains, the PTFs can be defined as the acoustic impedance of each patch, that is, the ratio between its mean pressure and its mean velocity. The PTFs should be estimated for each subsystem separately (cavity and set of SBHs). For an acoustic subsystem m, the PTF between patches i and j corresponds to a cross-impedance and is defined by,

$$Z_{ij}^m = \frac{\langle p_j^m \rangle}{\langle u_i^m \rangle}, \quad (1)$$

where $\langle p_j^m \rangle$ is the mean pressure on patch j when a mean normal velocity is imposed on patch i and all other patches have zero normal velocity. For the sake of brevity, the

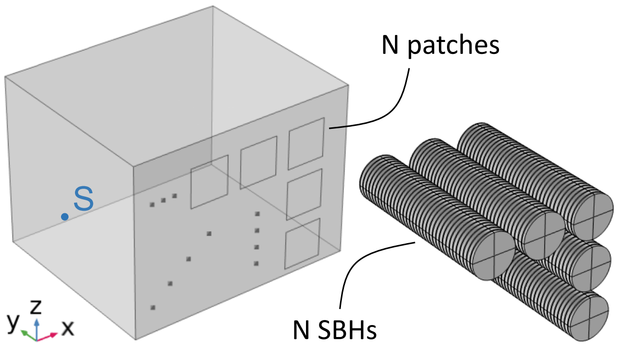

Figure 2. PTF sub-structuring of a cavity coupled to N SBHs.

brackets $\langle \quad \rangle$ will be hereby suppressed, and it is understood that all PTFs are defined from mean values.

Similarly, to account for an arbitrary receiver point R, the patch-to-point impedance is defined as

$$z_{Ri}^{m} = \frac{p(R)}{u_i^m}, \tag{2}$$

where $p(R)$ is the pressure at R when a mean normal velocity is imposed on patch i. Finally, the external source (i.e. the monopole at S in our case) is characterized by the patch blocked pressure p_{jS}^m, corresponding to the mean pressure on the patch j induced by the source when all other patches are rigid (null normal velocity), i.e.,

$$Z_{jS}^{m} = p_{jS}^{m}. \tag{3}$$

Once all the PTFs of interest for both subsystems have been calculated by any suitable method, we couple them to calculate the total system response by applying continuity conditions on the patches. In the following, we denote by $ss1$ the subsystem 1 (cavity) and by $ss2$ the subsystem 2 (N SBHs). Looking at Fig. 2, it is clear that the mean pressure in each patch will be the same for both the cavity and the SBHs, while the surface normal velocity will have opposite signs when pointing toward the cavity or toward the SBHs. Pressure and velocity continuity at each patch implies,

$$\begin{cases} p_j^{ss1} = p_j^{ss2} & \forall j = 1, ..., N \\ u_j^{ss1} = -u_j^{ss2} & \forall j = 1, ..., N. \end{cases} \tag{4}$$

The superposition principle allows one to compute the pressure at an arbitrary patch j of subsystem 1 as,

$$p_j^{ss1} = p_{jS}^{ss1} + \sum_{i=1}^{N} Z_{ij}^{ss1} u_i^{ss1} \quad \forall j = 1, ..., N, \tag{5}$$

and for subsystem 2 we have,

$$p_j^{ss2} = \sum_{i=1}^{N} Z_{ij}^{ss2} u_i^{ss2} \quad \forall j = 1, ..., N. \tag{6}$$

Applying the continuity condition of Eqn. 4 to Eqns. 5 and 6, we are left with the following matrix system that allows us to compute the coupling velocities in the patches from the impedances of subsystems 1 and 2 and the external pressure,

$$\left[u^{ss2}\right] = \left[Z^{ss1} + Z^{ss2}\right]^{-1} \left[p_S^{ss1}\right]. \tag{7}$$

2.2 Estimation of the PTFs of the cavity using the modal expansion method

The PTF method presents a substructuring strategy that does not depend on how the susbsytem impedances are calculated. Analytical, numerical or experimental approaches, or a mix of them, can be used [21]. In the present study, a modal expansion will be used for the cavity as it is rectangular and homogeneous.

The acoustic pressure inside the cavity admits a standard modal expansion,

$$p(x, y, z, \omega) = \sum_{q,r,s} \Gamma_{qrs}(\omega)\, \phi_{qrs}(x, y, z), \tag{8}$$

with eigenmodes,

$$\phi_{qrs}(x, y, z) = \cos\left(\frac{q\pi x}{L_x}\right) \cos\left(\frac{r\pi y}{L_y}\right) \cos\left(\frac{s\pi z}{L_z}\right), \tag{9}$$

and eigenfrequencies,

$$\omega_{qrs} = c_0 \sqrt{\left(\frac{q\pi}{L_x}\right)^2 + \left(\frac{r\pi}{L_y}\right)^2 + \left(\frac{s\pi}{L_z}\right)^2}. \tag{10}$$

The expansion coefficients $\Gamma_{qrs}(\omega)$ in Eqn. (8) are given by

$$\Gamma_{qrs} = \frac{\mathrm{j}\omega \int_{S_i} \phi_{qrs} dS}{\mu_{qrs}\left(-\omega^2 + \mathrm{j}\omega\eta_c\omega_{qrs} + \omega_{qrs}^2\right)}, \qquad \mu_{qrs} = \frac{L_x L_y L_z}{8\varepsilon_{qrs}\rho_0 c_0^2}. \tag{11}$$

In the above Equations c_0 is the speed of sound, $\mathrm{j} = \sqrt{-1}$, η_c is the modal damping factor and $\varepsilon_{qrs} = \left(\frac{1}{2}\right)^{\Xi}$, being Ξ the number of indices of the mode that equal zero.

From the modal expansion, we can compute the patch-to-patch impedance in Eqn. 1, needed to characterize the cavity (subsystem 1), as in Eqn. 12 below. Modal expressions from Eqns. 2 and 3 can be derived in a similar way,

$$Z_{ij}^{ss1} = -\sum_{q,r,s} \frac{\mathrm{j}\omega \int_{S_i} \phi_{qrs} dS \frac{1}{S_j} \int_{S_j} \phi_{qrs} dS}{\mu_{qrs}\left(-\omega^2 + \mathrm{j}\omega\eta_c\omega_{qrs} + \omega_{qrs}^2\right)}. \quad (12)$$

Note that, to ensure a reliable description of the cavity dynamics and considering that one patch is dedicated to each SBH, the number of vibration modes considered must be such that, for each propagation direction $q \geq N \frac{L_x}{L_x^{SBH}}$ and $r \geq N \frac{L_y}{L_y^{SBH}}$ [21].

2.3 Estimation of the SBH impedance using a FEM model

The SBH has been characterized by means of a FEM model to solve the wave equation using the commercial software COMSOL, see Fig. 3.

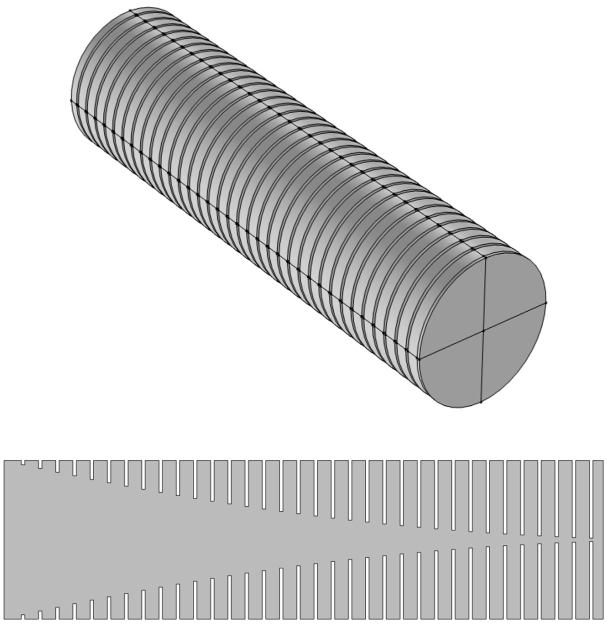

Figure 3. SBH model built in COMSOL: 3D and mid-plane cut view.

Given that we have neglected any interaction between the SBHs the impedance matrix of subsystem 2, Z^{ss2}, is diagonal. Furthermore, all the values on the diagonal will be equal to the impedance of a single SBH, Z_{SBH}, since we have considered all of them to be identical. Z_{SBH} is defined as the mean pressure on the SBH opening surface over the mean normal velocity prescribed at the opening. A unitary harmonic velocity is imposed at the entrance of the SBH FEM model, while the rings and external waveguide that comprises the SBH are considered rigid. By means of a direct FEM computation in the frequency domain, we obtain the pressure in the SBH aperture and get the impedance as,

$$Z_{SBH} = \frac{p_{SBH}}{u_{SBH}}. \quad (13)$$

Since the SBH has a retarding effect on the waves traveling through its interior, causing their effective wavelength λ_{eff} to diminish as the SBH termination is approached, a conservative criterion was established for the maximum mesh element size to be $h_{\max} \leq \lambda_{eff}/12$, where λ_{eff} is the minimum wavelength achieved inside the SBH. The SBH domain was meshed using tetrahedral elements.

2.4 Coupling of the subsystems and computation of the mean quadratic pressure

Having obtained the impedance matrices for subsystems 1 and 2 in the previous sections, we can now compute the mean velocities at the patches from Eqn. 7. Next, it is straightforward to calculate the acoustic pressure at any receiver point inside the cavity, $R \in \Omega_c$, as

$$p(R) = p_S^{ss1}(R) + \sum_{i=1}^{N} z_{Ri}^{ss1} u_i. \quad (14)$$

The mean square sound pressure inside the cavity is finally obtained by averaging over the cavity volume,

$$\left\langle p^2 \right\rangle^{ss1} = \frac{1}{\Omega_c} \int_{\Omega_c} p(R)\, \bar{p}(R)\; \mathrm{d}\Omega_c, \quad (15)$$

with $\Omega_c = L_x L_y L_z$ and the overbar denoting the complex conjugate.

3. VALIDATION OF THE PTF STRATEGY AGAINST FEM

To validate the proposed PTF method for the current cavity plus SBH problem, a first case study was conducted.

Fig. 4 shows the tested case. This comprises an air cavity of dimensions $0.24 \times 0.20 \times 0.18$ m^3 and a monopole source located at $(0.034,\ 0.16,\ 0.36)$ m with volume velocity 10^{-6} m^3/s. The air has density $\rho_0 = 1.297$ kg/m^3, sound speed $c_0 = 340$ m/s and damping $\eta_{ss1} = 0.01$. The two SBHs in the model are identical and have a quadratic profile with entrance radius $R_0 = 23$ mm, length $L = 0.175$ m, truncation $l = 1$ mm, 35 rings of thickness $h_r = 1$ mm and minimum radius at truncation $r_l = 0.5$ mm. Viscothermal losses inside the SBHs are accounted for by means of a constant damping factor $\eta_{ss2} = 0.05$. The two SBHs are positioned on the plane xz at coordinates $a = (0.192,\ 0.135)$ m and $b = (0.048,\ 0.045)$ m. The cut-on frequency of a quadratic SBH is given by $f_{\text{cut-on}} = c_0/\pi L \sim 618$ Hz [24] while the cut-off frequency of the duct, beyond which non-planar waves propagate, is extremely high in this case given the small radius of the duct $f = 1.84c_0/R_0 \sim 27.4 \times 10^3$. Results will be presented for the frequency range between 600 and 2000 Hz.

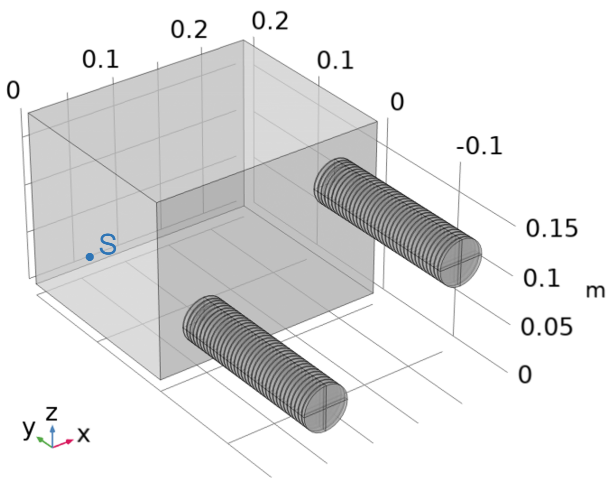

Figure 4. Nominal system to validate the proposed method.

From the SBH impedance obtained in Section 2.3, we can compute the reflection coefficient, R,

$$\mathrm{R} = \frac{Z_{SBH} - Z_0}{Z_{SBH} + Z_0}, \tag{16}$$

where $Z_0 = \rho_0 c_0$ is the characteristic impedance of air. The absorption coefficient, α, is given by,

$$\alpha = 1 - \left|\mathrm{R}^2\right|, \tag{17}$$

and has been represented in Fig. 5. As seen, its values are very close to 1 for the analyzed frequency range.

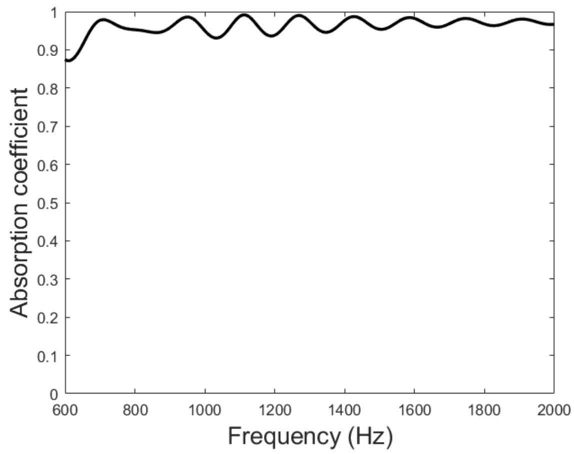

Figure 5. Absorption coefficient of the SBH.

Finally, the complete coupled system (subsystem 1 + subsystem 2) has been modelled using a FEM model and is taken as a reference for comparison with the proposed PTF substructuring methodology. In Fig. 6, we present the mean square sound pressure of the cavity (see Eqn. (15)) without SBHs (black line), with SBHs using the complete FEM model (dashed blue line) and with SBHs using the PTF approach (dashed orange line). The influence of the SBHs on the cavity is very significant for all modes, as it is clearly observed. Surprisingly, for higher frequencies, where the coefficient α remains very high, the influence of the SBHs seems to be less important than at lower frequencies. This is attributed to the fact that the SBHs are located close to the nodal planes of the involved modes.

As for the comparison between the proposed PTF method and the FEM complete model, it is seen that the mean error over the analyzed range is 0.58 dB and that the maximum observed error is $\sim$ 3 dB at 1400 Hz. The FEM model has 345579 elements and took 105 minutes to compute, while the PTF, coded and simulated in Matlab, took only 0.5 seconds.

4. CONCLUSIONS

In this work, a numerical procedure based on patch transfer functions (PTFs) was presented to calculate the response of a closed cavity coupled to sonic black holes (SBHs) when an inner sound source is excited. The cavity

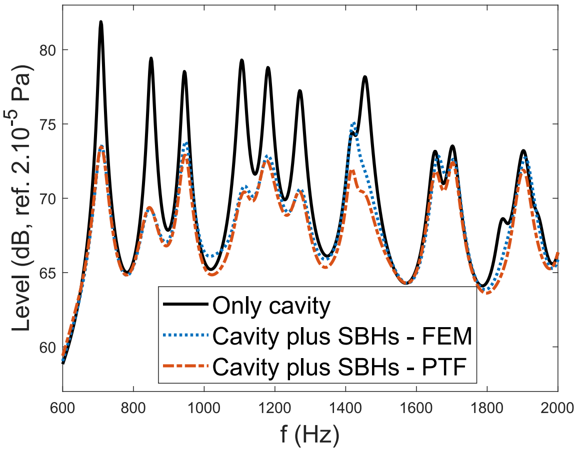

Figure 6. Mean quadratic pressure inside the cavity - Validation.

plus SBHs system was divided into a cavity subdomain and an SBHs subdomain. The former was characterized by means of a modal expansion while a FEM model was used for the SBHs. Also a FEM model of the complete system was built for comparison. The comparison between the latter and the proposed PTF approach shows a very good agreement, and that the PTF requires much less calculation time.

Given the efficiency of the presented approach, in future work it will be easy to test different and optimal distributions of SBHs in cavity walls, as well as to improve their modelling for better characterization. Different types of SBHs, such as those cited in the introduction with, for example, improved behavior at low frequency, could also be easily tested in the proposed framework.

5. REFERENCES

[1] A. Pelat, F. Gautier, S. Conlon, and F. Semperlotti, "The acoustic black hole: A review of theory and applications," *Journal of Sound and Vibration*, p. 115316, Mar 2020.

[2] M. Mironov, "Propagation of a flexural wave in a plate whose thickness decreases smoothly to zero in a finite interval," *Soviet Physics Acoustics*, vol. 34, no. 3, pp. 318–319, 1988.

[3] V. Krylov and F. Tilman, "Acoustic 'black holes' for flexural waves as effective vibration dampers," *Journal of Sound and Vibration*, vol. 274, no. 3, pp. 605–619, 2004.

[4] M. Mironov and V. Pislyakov, "One-dimensional acoustic waves in retarding structures with propagation velocity tending to zero," *Acoustical Physics*, vol. 48, 05 2002.

[5] J. Deng, O. Guasch, and D. Ghilardi, "Solution and analysis of a continuum model of sonic black hole for duct terminations," *Applied Mathematical Modelling*, vol. 129, pp. 191–206, 2024.

[6] O. Guasch, M. Arnela, and P. Sánchez-Martín, "Transfer matrices to characterize linear and quadratic acoustic black holes in duct terminations," *Journal of Sound and Vibration*, vol. 395, pp. 65–79, 2017.

[7] M. Červenka and M. Bednařík, "On the role of resonance and thermoviscous losses in an implementation of "acoustic black hole" for sound absorption in air," *Wave Motion*, vol. 114, p. 103039, 2022.

[8] S. Li, J. Xia, X. Yu, X. Zhang, and L. Cheng, "A sonic black hole structure with perforated boundary for slow wave generation," *Journal of Sound and Vibration*, vol. 559, p. 117781, 2023.

[9] A. Mousavi, M. Berggren, and E. Wadbro, "How the waveguide acoustic black hole works: A study of possible damping mechanisms," *The Journal of the Acoustical Society of America*, vol. 151, no. 6, pp. 4279–4290, 2022.

[10] O. Umnova, D. Brooke, P. Leclaire, and T. Dupont, "Multiple resonances in lossy acoustic black holes - theory and experiment," *Journal of Sound and Vibration*, vol. 543, p. 117377, 2023.

[11] X. Zhang and L. Cheng, "Broadband and low frequency sound absorption by sonic black holes with micro-perforated boundaries," *Journal of Sound and Vibration*, vol. 512, p. 116401, 2021.

[12] Y. Chen, K. Yu, Q. Fu, J. Zhang, X. Lu, X. Du, and X. Sun, "A broadband and low-frequency sound absorber of sonic black holes with multi-layered micro-perforated panels," *Applied Acoustics*, vol. 217, p. 109817, 2024.

[13] Y. Mi, L. Cheng, W. Zhai, and X. Yu, "Broadband low-frequency sound attenuation in duct with embedded periodic sonic black holes," *Journal of Sound and Vibration*, vol. 536, p. 117138, 2022.

[14] J. Deng and O. Guasch, "Sound waves in continuum models of periodic sonic black holes," *Mechanical Systems and Signal Processing*, vol. 205, p. 110853, 2023.

[15] G. Serra, O. Guasch, M. Arnela, and D. Miralles, "Optimization of the profile and distribution of absorption material in sonic black holes," *Mechanical Systems and Signal Processing*, vol. 202, p. 110707, 2023.

[16] A. Mousavi, M. Berggren, L. Hägg, and E. Wadbro, "Topology optimization of a waveguide acoustic black hole for enhanced wave focusing," *The Journal of the Acoustical Society of America*, vol. 155, no. 1, pp. 742–756, 2024.

[17] O. Guasch, P. Sánchez-Martín, and D. Ghilardi, "Application of the transfer matrix approximation for wave propagation in a metafluid representing an acoustic black hole duct termination," *Applied Mathematical Modelling*, vol. 77, pp. 1881–1893, 2020.

[18] M. Mironov and V. Pislyakov, "One-dimensional sonic black holes: Exact analytical solution and experiments," *Journal of Sound and Vibration*, vol. 473, p. 115223, 2020.

[19] J. W. Chua, X. Li, X. Yu, and W. Zhai, "Novel slow-sound lattice absorbers based on the sonic black hole," *Composite Structures*, vol. 304, p. 116434, 2023.

[20] T. Bravo and C. Maury, "Broadband sound attenuation and absorption by duct silencers based on the acoustic black hole effect: Simulations and experiments," *Journal of Sound and Vibration*, vol. 561, p. 117825, 2023.

[21] M. Ouisse, L. Maxit, C. Cacciolati, and J.-L. Guyader, "Patch transfer functions as a tool to couple linear acoustic problems," *Journal of Vibration and Acoustics*, vol. 127, 10 2005.

[22] L. Maxit, M. Aucejo, and J.-L. Guyader, "Improving the patch transfer function approach for fluid-structure modelling in heavy fluid," *Journal of Vibration and Acoustics*, vol. 134, p. 051011, 10 2012.

[23] T. Zhong and C. Yang, "Application of the patch transfer function method for predicting flow-induced cavity oscillations," *Journal of Sound and Vibration*, vol. 521, p. 116678, 2022.

[24] Y. Mi, W. Zhai, L. Cheng, C. Xi, and X. Yu, "Wave trapping by acoustic black hole: Simultaneous reduction of sound reflection and transmission," *Applied Physics Letters*, vol. 118, no. 11, 2021.